

# Improved representation of retinal data acquired with volumetric Fd-OCT: co-registration, visualization and reconstruction of a large field of view

Robert J. Zawadzki\*<sup>a</sup>, Alfred R. Fuller<sup>b</sup>, Stacey S. Choi<sup>a</sup>, David F. Wiley<sup>b,c</sup>,  
Bernd Hamann<sup>b,c</sup> and John S. Werner<sup>a</sup>

<sup>a</sup> Vision Science and Advanced Retinal Imaging Laboratory (VSRI), Dept. of Ophthalmology & Vision Science, UC Davis, 4860 Y Street, Suite 2400, Sacramento, CA, USA 95817;

<sup>b</sup> Visualization and Computer Graphics Research Group, Institute for Data Analysis and Visualization (IDAV), UC Davis, One Shields Avenue, Davis, CA 95616;

<sup>c</sup> Stratovan Corporation, Woodland, CA

## ABSTRACT

Advances in Fourier-domain optical coherence tomography (Fd-OCT) permit visualization of three-dimensional morphology of in-vivo retinal structures in a way that promises to revolutionize clinical and experimental imaging of the retina. The relevance of these advances will be further increased by the recent introduction of several commercial Fd-OCT instruments that can be used in clinical practice. However, due to some inherent limitations of current Fd-OCT technology (e.g., lack of spectroscopic information, inability to measure fluorescent signals), it is important to co-register Fd-OCT data with images obtained by other clinical imaging modalities such as fundus cameras and fluorescence angiography to create a more complete interpretation and representation of structures imaged. The co-registration between different imaging platforms becomes even more important if small retinal changes are monitored for early detection and treatment. Despite advances in volume acquisition speed with FD-OCT, eye/head motion artifacts can be still seen on acquired data. Additionally high-sampling density, large field-of-view (FOV) Fd-OCT volumes may also be needed for comparison with conventional imaging. In standard Fd-OCT systems, higher sampling density and larger imaging FOV (with constant sampling densities) lead to longer acquisition time which further increases eye/head motion artifacts. To overcome those problems, we tested 3D stitching of multiple, smaller retinal volumes which can be acquired in a less time (reduction of motion artifacts) and/or when stitched create a larger FOV representation of the retina. Custom visualization software that makes possible manual co-registration and simultaneous visualization of volumetric Fd-OCT data sets is described. Volumetric visualizations of healthy retinas with corresponding fundus pictures are presented followed by examples of retinal volumes of high sampling density that are created from multiple "standard" Fd-OCT volumes.

**Keywords:** (110.4500) Optical coherence tomography; (170.0110) Imaging system; (170.4470) Ophthalmology; (120.3890) Medical optics instrumentation

## 1. INTRODUCTION

Acquisition speed of current Fourier-domain optical coherence tomography (FD-OCT) systems [1-3] allows measurements of volumetric retinal structures within 2 to 10 seconds, depending on the system's speed and lateral sampling density. Therefore volumetric representation of the retina, as in other medical areas, is becoming an increasingly important tool for ophthalmic clinical diagnosis and research. The Fd-OCT system described in this paper was constructed at the UC Davis Medical Center on a small laboratory optical bench, and its detail is described elsewhere [4-5]. Data acquisition software developed by Bioptigen Inc. (Durham, NC.), processes, displays and streams B-scan data to system memory in real time at the same frame rates.

\*rjzawadzki@ucdavis.edu; phone: 1-916-734-5839; fax: 1-916-734-4543; web: <http://vsri.ucdavis.edu>

The process includes re-sampling from  $\lambda$  to  $k$ , dispersion compensation to third order and FFT. In addition, a real-time OCT en-face view is displayed, allowing the operator to track and eliminate streamed data affected by eye motion or blinking. To reduce head motion, an assembly of a bite-bar and a forehead-rest mounted on an X-Y-Z translation stage is used. This also makes possible precise positioning of the subject's eye with respect to the imaging light. An external fixation target is used to further minimize eye motion and to allow precise imaging of different retinal locations. To minimize axial distortions (mainly due to head motion) and lateral distortions (mainly due to eye motion) between consecutive B-scans we use Image J - based registration software, where 2D cross correlation is used to calculate lateral and axial displacement between two consecutive B-scans [6-7]. Volume stitching and co-registration methods presented in this paper are a part of our custom volumetric visualization and segmentation software. The results of image data manipulation are immediately visualized by our volume rendering software. We think that these tools may find further application in temporal monitoring of retinal disease as well as for comparisons between imaging modalities as well as across OCT platforms.

## 2. MATERIALS AND METHODS

The volumetric retinal data presented in this paper have been acquired by our clinical Fd-OCT system developed at UC Davis in collaboration with Duke University. This instrument has been already described in our previous reports [5]. The configuration used here uses a superluminescent diode (855@75nm) from Superlum allowing 4.5  $\mu$ m axial resolution of the retina ( $n=1.38$ ). Measured power at the subject's eye was equal to 700  $\mu$ W. With our current spectrometer design, the maximum axial range (seen after the Fourier transform) is 2.7 mm in free space and around 2 mm in the eye. So far more than 350 subjects, with healthy and diseased eyes, have been imaged with this clinical instrument.

### 2.1. Volumetric data acquisition

Several different 3D raster scanning modes have been used to acquire the images presented in this paper. In our standard sampling acquisition mode (100 B-scans (1000 lines/B-scan)) where 100,000 A-lines are acquired it takes about  $T_{reg}=5.5s$  to image one volume (with line acquisition exposure of 50  $\mu$ s). This time ( $T_{reg}$ ) is of course system dependent, but we will use it as reference for comparison of different acquisition modes. An alternative commonly used sampling grid: (200 B-scans (500 lines/B-scan)) requires the same acquisition time  $T_{reg}$ . Unfortunately, despite head restraint and implementation of B-scan co-registration all the eye and motion distortions cannot be corrected. This can be observed as distortions in retinal vasculature on the OCT fundus image [8] (reconstructed from Volumetric data). One way to minimize this problem is tracking and correcting for retinal motion that can be achieved by actively correcting eye motions in real time during acquisition [9] or in post processing step [10]. Application of any of these methods would require construction of new more complex and probably more costly imaging instruments and will not be discussed in this manuscript. Another natural way to reduce distortion artifacts includes reduction of volume acquisition time  $T_{reg}$ . This can be achieved by shortening A-line exposure. In a mean time however there are also another ways to minimize motion distortions for existing FD-OCT systems. One includes reduction of volumetric grid sampling density (e.g., reduction of total A-lines by factor of 2 would reduce  $T_{reg}$  by the same amount). Unfortunately this also means reduction in quality of retinal volumes. Another method for minimizing motion distortions, that we explore in this paper, includes acquisition of multiple smaller volumes that can be stitched together to create standard or high sampling density volumes. Table 1 compares acquisition times and sampling densities of sub-volumes that were tested in this paper.

Table 1. Comparison of volume acquisition times for standard volumes and 4 sub-volumes.

<b><u>Standard Volume:</u></b>	<b><u>Regular density sub-volumes:</u></b>	<b><u>High density sub-volumes:</u></b>
<u>Sampling grid:</u> (100,000 lines)	<u>Sampling grid:</u> (36,000 lines)	<u>Sampling grid:</u> (72,000 lines)
100 B-scans; 1000 lines/B-scan 200 B-scans; 500 lines/B-scan	60 B-scans; 600 lines/B-scan  <u>Stitched grid (x4):</u> (100,000 lines) 100 B-scans; 1000 lines/B-scan	120 B-scans; 600 lines/B-scan  <u>Stitched grid (x4):</u> (200,000 lines) 200 B-scans; 1000 lines/B-scan
<u>Acquisition time:</u> $T_{reg}$	<u>Acquisition time:</u> 36 % $T_{reg}$	<u>Acquisition time:</u> 72 % $T_{reg}$
<u>Total Time:</u> $T_{reg}$	<u>Total Time:</u> 144 % $T_{reg}$	<u>Total Time:</u> 288% $T_{reg}$

### 2.1.1. Acquisition of sub-volumes.

As shown in Table 1 we tested two sets of sub-volumes, one resulting in our standard density volume and the other resulting in a high- density volume. For reference standard volumes have been acquired over a 5x5mm area; in the case of four sub-volumes acquisition single sub-volume was set to cover 3x3mm that resulted in overlapping of multiple sub-volumes as shown by Figure 1. Assuming that overlapping areas equals about 30 % of all sub-volumes we end up with sampling grid of 100,000 A-scans for standard and 200,000 A-scans for high resolution sub-volumes. Respectively due to the reduction of the number of sampling points in single sub-volumes it takes only 36% of the reference time to acquire one standard sub-volume and 72% to acquire one high density sub-volume. This reduction of single volume acquisition time without scarifying resolution of final volume is the biggest advantage of this method.

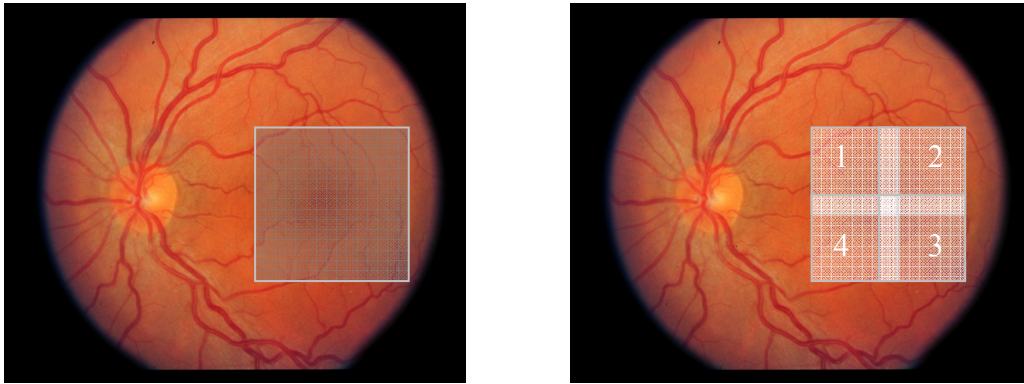


Fig. 1: An example of OCT scanning areas of volumetric measurements. Left: standard volume acquisition area; Right: location of the four sub-volumes acquisition area. Numbers on the sub-volumes refer to the order in which they were acquired. Fundus photo is used for reference.

There are two ways to acquire sub-volumes that may be used to create a larger volume. One is done by changing the location of the subject's fixation point. Another can be achieved by keeping subject fixation in one position and changing driving voltages of the scanners to cover different retinal locations. The figure below is a schematic drawing of both methods.

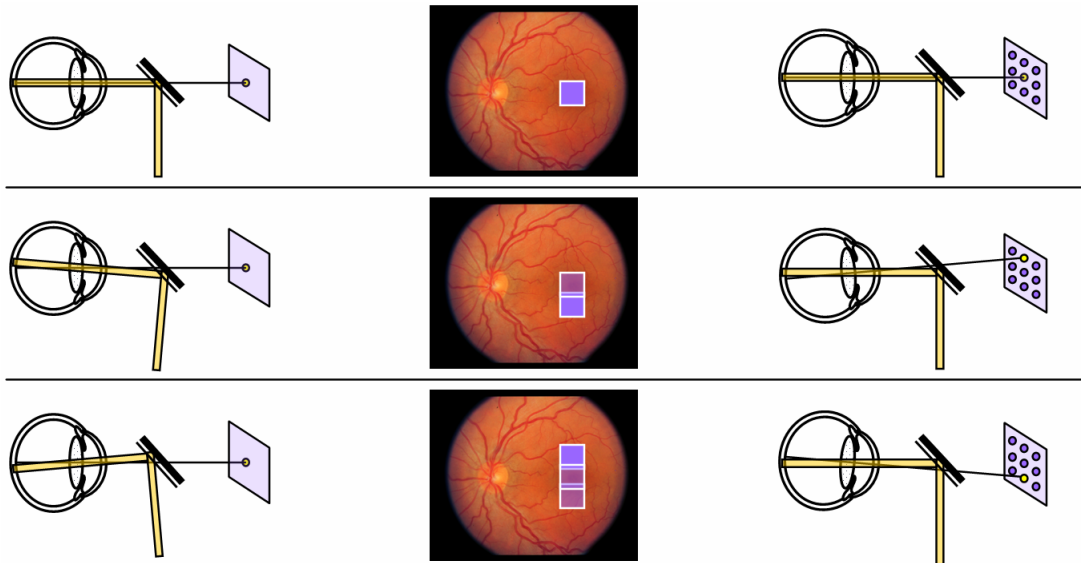


Fig. 2: Two examples of sub-volume acquisition schemes. Left: one fixation point, location of the volume set by scanning instrument; Middle: Retinal location of acquired sub-volume; Right: multiple fixation points, location of the volume is set by fixation point.

In general first method (with one fixation point) requires an imaging system with a large FOV. This is very often a limiting factor that forces use of the second method (changing of fixation point). In this paper we tested both sub-volume acquisition methods.

### 2.1.2. Stitching and visualization of sub-volumes.

In order to be able to stitch sub-volumes we have built-in an additional functionality into our OCT Volume Renderer, described previously [11], that allows active manipulation and viewing of the resulting volume and its cross sectional slices in real time. In our current system we can freely translate volumes in three dimensions. These data can be than stitched and saved as a single large volume. There are various ways of combining the data in the overlapping regions. We currently choose the maximum value of two overlaying voxels as value of resulting voxel in order to preserve the prominent characteristics of each volume. The figure below shows a schematic of the volume manipulation allowed during sub-volume registration.

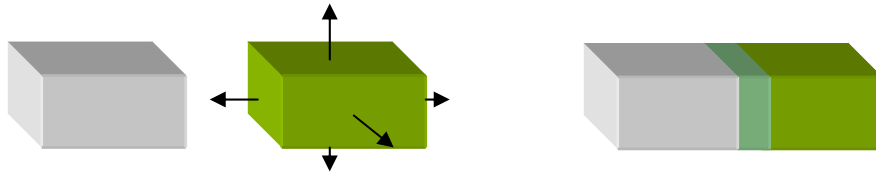


Fig. 3: Left: Schematic of the Volume manipulation allowed during volume stitching in our Volume Renderer. Right: Resulting volume with “shared” Voxels.

## 2.2. Co-registration of OCT volumetric data sets with other imaging modalities

As already pointed out due to the growing reliance on FD-OCT in ophthalmological diagnoses, it is increasingly important to be able to compare results obtained with this instrument to other clinical systems. This task is trivial if the OCT instrument itself is a part of such a system. Otherwise cross platform registration needs to be implemented. This problem is quite complex as the scaling and distortions between imaging platforms may not be linear. In this work however we will present simplified co-registration that allows only scaling, translation and rotation of co-registered image.

### 2.2.1. Co-registration with fundus photos.

Similarly to the aforementioned stitching and visualization of sub-volumes, we have build-in an additional functionality into our OCT Volume Renderer [11], that allows active manipulation and viewing of a co-registered images on the corresponding OCT volume, its OCT fundus and cross sectional slices. In our current system we can freely scale, rotate and translate a fundus photo in three dimensions. All this manipulation is done with the co-registered image only (OCT data remains un-changed). This approach allows the segmentations and annotations imposed on the OCT volume to be displayed on the co-registered fundus photo. Figure 4 shows a schematic of the volume manipulation allowed during this registration process.

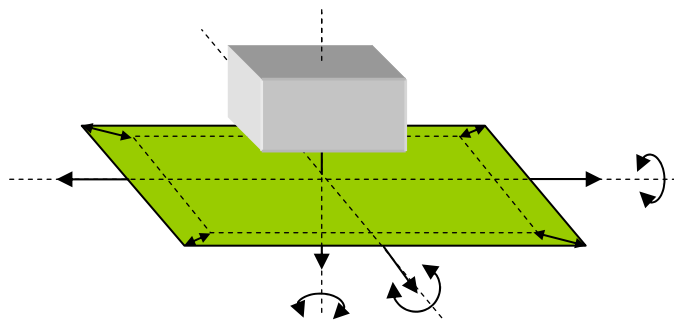


Fig. 4: Schematic of the manipulation allowed during co-registration of the fundus photo with the OCT volume.

### 3. RESULTS

We tested our stitching and co-registration methods using multiple data sets acquired on the same subject's fovea and optic nerve head (ONH). Similarly to our previous sections our results will be divided into two subsections, one concerning sub-volume acquisition and stitching, and the second about OCT volume and fundus photo co-registration.

#### 3.1. Stitching of multiple sub-volumes.

To visualize the effectiveness of our volume stitching software, a volumetric rendering of the four sub-volumes acquired over the fovea both before and after stitching is presented in Figure 5.

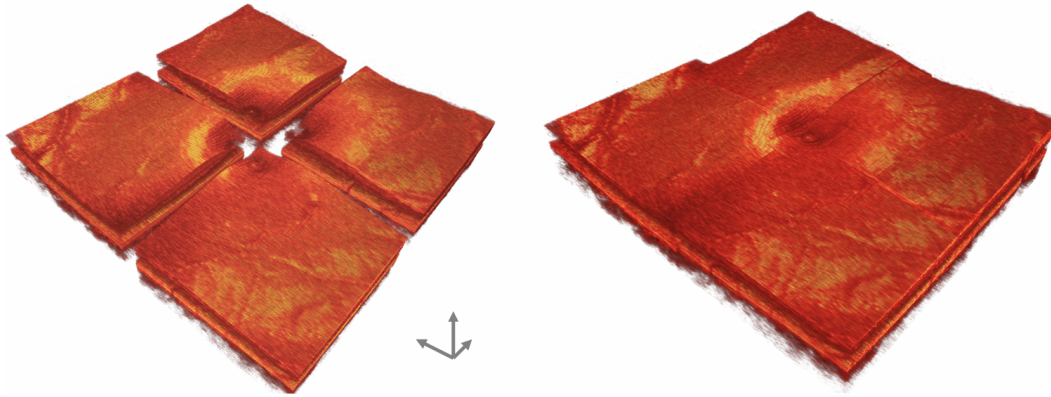


Fig. 5. Visualization of the 4 sub-volumes before (left) and after stitching (right).

Next, we compared large volumes obtained from stitching of four sub-volumes acquired with a fixed or changing fixation point. The figure below shows the resulting volumes of each method. The final volume covers about a 5x5mm area while the four sub volumes each cover a 3x3mm area. It can be seen that the volume obtained with a changing fixation point has more distortions (non-matched structures in sub-volumes) probably due to the change in the eye shape when looking in different directions.

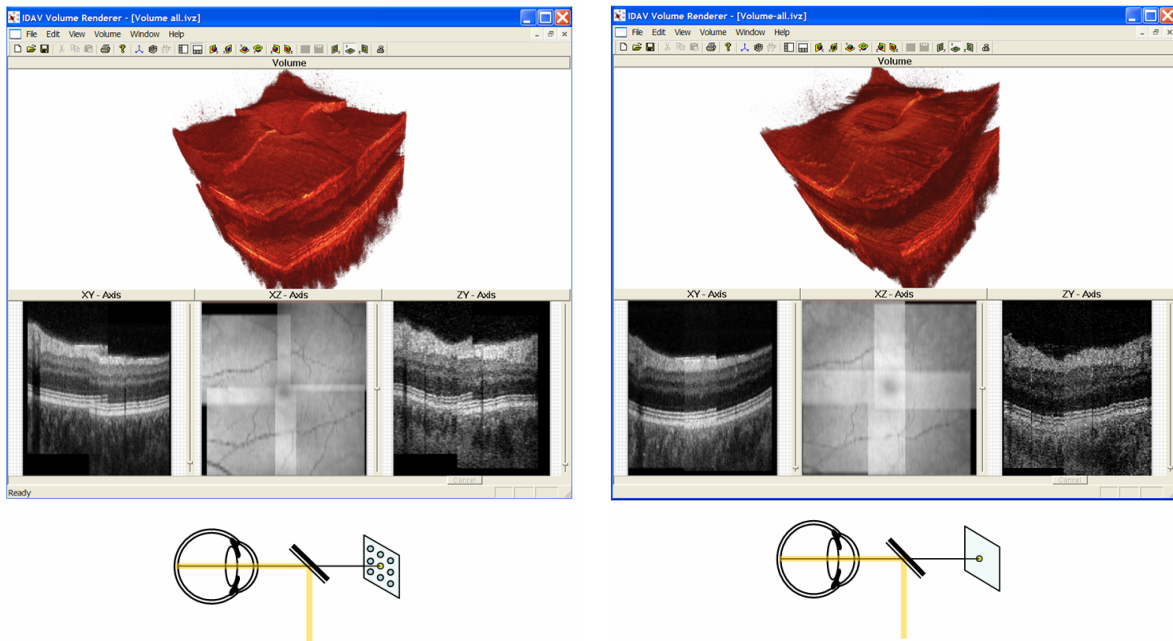


Fig. 6. Visualization of volume stitching with sub-volumes acquired with two different methods. Left: Sub-volumes acquired with changing fixation point; Right: Sub-volumes acquired with one fixation point and scanning location adjusted in the instrument.

As can be clearly seen on the cross-sectional slices shown above, sub-volumes acquired with a changing fixation point have more cross sub-volume distortions than one acquired using a single fixation point. However even in second case distortions are still present suggesting that more complex volume manipulations are needed for better sub-volume registration. To compare our sub-volume acquisition method to our standard volume acquisition one, we imaged the ONH of a healthy subject. We chose the sub-volume acquisition with one fixation point as the one resulting in less distortion. Figure 7 below shows the result of this comparison.

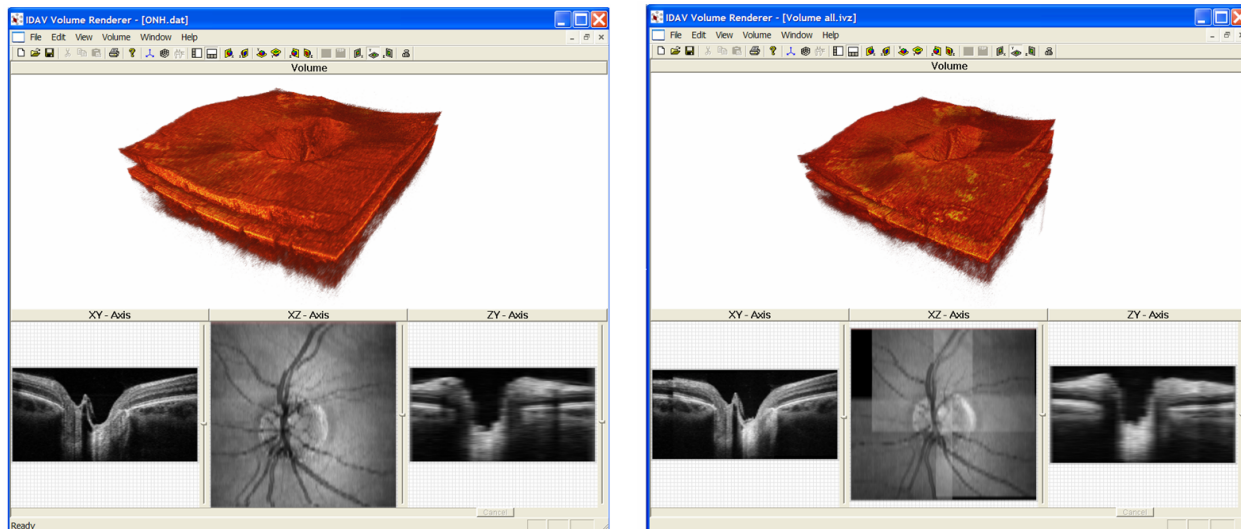


Fig. 7. Comparison of single volume acquisition (left) and multiple volume acquisition (right) acquired over ONH region.

Importantly, note that there is virtually no lateral motion artifact on the OCT fundus reconstructed from the stitched sub-volumes compared to small lateral distortions seen on single volume acquisition.

### 3.2. Co-registration of OCT volumes to fundus photo.

To visualize the performance of our co-registration and visualization software, Figure 8 shows a foveal OCT volume co-registered with the same subject’s fundus photo (taken with a clinical fundus camera).

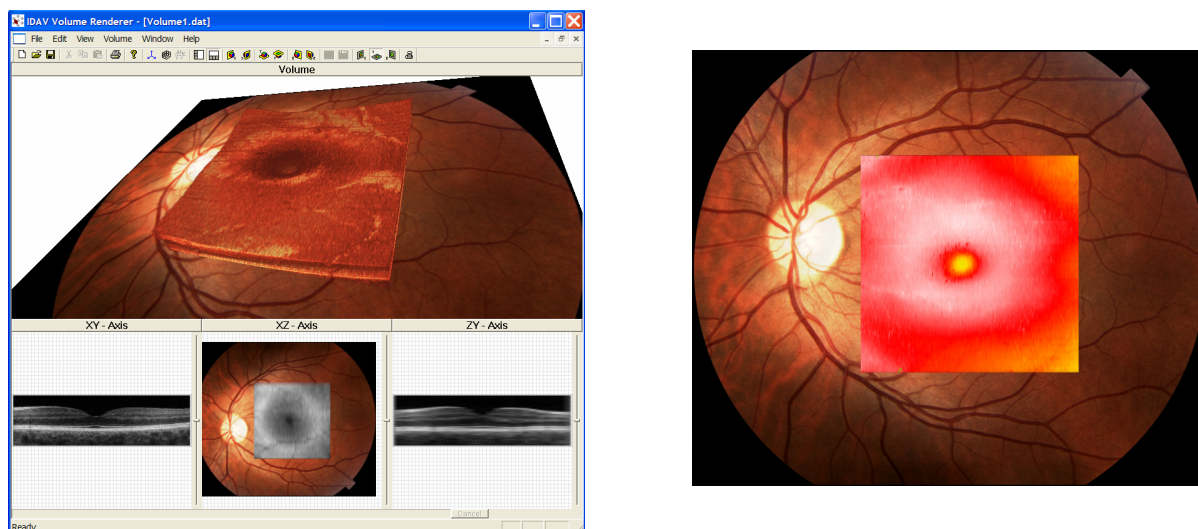


Fig. 8. Visualization of the OCT volume co-registered to the clinical fundus photo. Left: Screen shot from our Volume Rendering software; Right: Thickness map of total retinal thickness, segmented with our SVM segmentation code superimposed on the fundus photo after co-registration shown in the left panel.

As presented in the figure above, one of the main advantages of co-registering fundus photos within our Volume Render is easy transfer and visualization of segmentations and drawing annotations done on the original OCT volume. Another example of this feature is also shown in Figure 9, where drawing annotations done on the OCT fundus image can be visualized on the clinical fundus photo.

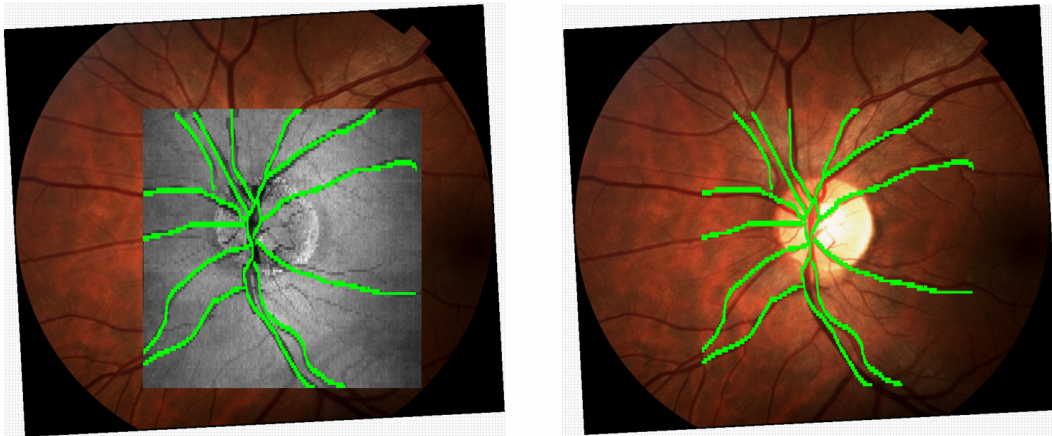


Fig. 9. Left: Visualization of the OCT fundus co-registered to fundus photo with green lines drawn over vascular pattern as seen with OCT fundus. Right: result of the drawings from left figure overlaid with fundus photo (without OCT fundus).

We think that this feature may prove to be very useful in clinical application where comparing features seen with different imaging modalities is very important for comprehensive assessment.

To illustrate some of the problems that still need to be addressed in further development of co-registration between OCT volumes and fundus photos, we show a side view of the volumes in the figure below.

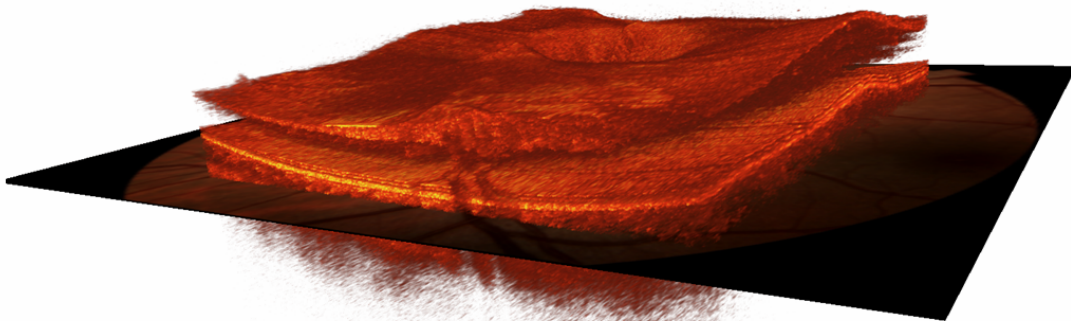


Fig. 10. Side view of the OCT volume of ONH (from fig. 9.) co-registered with fundus photo.

As seen above clear mismatch between the shape of the volume and that of the fundus photo can be observed. This suggests that one should limit viewing of co-registered volumes and fundus photos to *en-face* views (from above) until additional algorithms are developed). Different methods of fundus visualization are clearly needed for side view of the volumes.

#### 4. CONCLUSIONS

Two methods to enhance performance and clinical applicability of our Fd-OCT system have been presented. One includes possible reduction of motion artifacts by acquiring multiple sub-volumes in shorter acquisition time and its later stitching to create one volume. The second method focuses on co-registration of OCT volumes to the fundus photos and includes visualization of OCT data and results of its manipulation that can be viewed directly on the fundus photo. The practical impact of these methods still needs to be verified. However, in our opinion they may allow better use of

existing instrumentation as well as visualization of results acquired with OCT and its presentation in the format that facilitates clinical interpretation and research.

## ACKNOWLEDGEMENTS

We gratefully acknowledge the contributions of Joseph A. Izatt from the Department of Biomedical Engineering, Duke University Durham, NC. The help of Bioptigen Inc. for providing OCT data acquisition software is appreciated. This research was supported by the National Eye Institute (EY 014743). Alfred Fuller has been supported by a Student Employee Graduate Research Fellowship (SEGRF) from Lawrence Livermore National Laboratory.

## REFERENCES

1. M. Wojtkowski, T. Bajraszewski, P. Targowski and A. Kowalczyk „ Real time in vivo imaging by high-speed spectral optical coherence tomography”, *Opt. Lett.* **28**, 1745-1747 (2003)
2. R. Leitgeb, C.K. Hitzenberger, and A.F. Fercher “Performance of fourier domain vs. time domain optical coherence tomography”, *Opt. Express* **11**, 889-894 (2003)
3. N.A. Nassif, B. Cense, B.H. Park, M.C. Pierce, S.H. Yun, B.E. Bouma, G.J. Tearney, t.C. Chen, J.F. de Boer “In vivo high-resolution video-rate spectral-domain optical coherence tomography of the human retina and optic nerve”, *Opt. Express* **12**, 367-376 (2004)
4. R.J. Zawadzki, S. Jones, S. Olivier, M. Zhao, B. Bower, J. Izatt, S. Choi, S. Laut, and J. Werner, "Adaptive-optics optical coherence tomography for high-resolution and high-speed 3D retinal in vivo imaging," *Opt. Express* **13**, 8532-8546 (2005)
5. R.J. Zawadzki, A.R. Fuller, D.F. Wiley, B. Hamann, S.S. Choi, J.S. Werner, “Adaptation of a support vector machine algorithm for segmentation and visualization of retinal structures in volumetric optical coherence tomography data sets,” *Journal of Biomedical Optics* **12**, 041206 (1-8) (2007)
6. <http://rsb.info.nih.gov/ij/>
7. <http://bigwww.epfl.ch/thevenaz/turboreg/>
8. S. Jiao, R. Knighton, X. Huang, G. Gregori, and C. Puliafito, "Simultaneous acquisition of sectional and fundus ophthalmic images with spectral-domain optical coherence tomography," *Opt. Express* **13**, 444-452 (2005)
9. R. D. Ferguson, D. X. Hammer, L. A. Paunescu, S. Beaton, and J. S. Schuman, "Tracking optical coherence tomography," *Opt. Lett.* **29**, 2139-2141 (2004)
10. S.B. Stevenson, A. Roorda, “Correcting for miniature eye movements in high-resolution scanning laser ophthalmoscopy,” *BiOS 2007 Proc. SPIE Vol.* **5688**, p.145-151 (2005)
11. A.R. Fuller, R.J. Zawadzki, S.S. Choi, D.F. Wiley, J.S. Werner and B. Hamann, “Segmentation of three-dimensional retinal image data, “ in: Chen, M., Hansen, C.D. and Pang, A., eds., *IEEE Visualization 2007, IEEE Transactions on Visualization and Computer Graphics* **13** (2007)